Site-Specific Seismic Hazard Assessment and Ground Motion Selection for Nonlinear Time History Analysis

Faradina Safiraa[a], Yuyun Tajunnisa[a], M. Sigit Darmawan[a] ,Hendra Wahyudi[a]

[a]*Department of Civil Infrastructure Engineering, Sepuluh Nopember Institute of Technology, Surabaya, 60116, Indonesia*
Corresponding author: yuyun_t@its.ac.id

Abstract
This journal aims to study a comprehensive methodology involving Deterministic Seismic Hazard Analysis (DSHA), site-specific ground motion selection, spectral matching, and nonlinear dynamic analysis on Beribis Kendeng Waleri Fault. Seven strong ground motion records were selected from the PEER NGA-West2 database and spectrally matched to the target response spectrum derived from DSHA parameters. Local site effects were incorporated through a site response analysis using detailed subsurface soil data, which classified the site as Class E (very soft soil). The resulting surface-level acceleration time histories were used in nonlinear time history analysis to assess structural performance.

Keywords: DSHA, Time history analysis, Site-specific response, Seismic performance evaluation, Spectral matching

1. Introduction

The geographical position of the Indonesian Archipelago is in the Pacific Ring of Fire / Pacific Ring of Fire Belt Area with a series of volcanoes along 40,000 km with a total of 452 mountains. In the Pacific Ring of Fire belt area, there is a meeting of three large tectonic plates, namely the Eurasian Plate, the Indo-Australian Plate, and the Pacific Plate [1]. The result of the meeting of these three plates causes the growth of a row of volcanoes along the islands of Java-Bali-Nusa Tenggara, Sumatra, Sulawesi-Malaku, and ending in Papua. These plates are actively moving and colliding with each other in Indonesia, which can cause earthquakes as seen in Figure 1 [1]. A crucial element in earthquake geology research is carefully mapping the locations of active earthquake-producing fault lines, based on the morphological features of their movement and the Quaternary deposits within their deformation zones. Then, based on estimates of the age of the deformed deposits and the magnitude of their displacement, earthquake parameters can be calculated: the fault slip rate, the magnitude of the displacement or thrust of each earthquake, and the age of the earthquake [1].

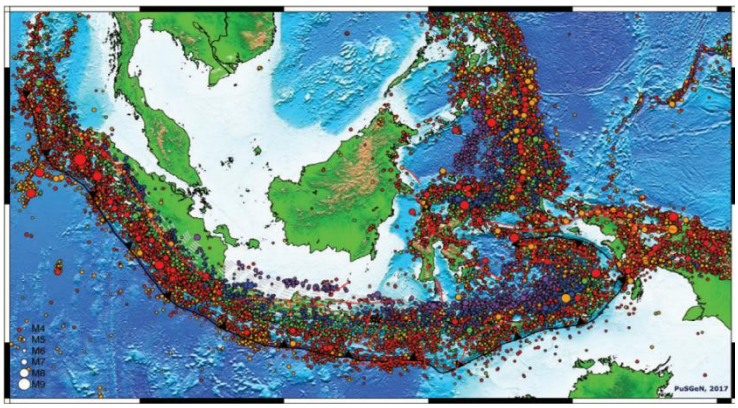

Figure 1. Earthquakes in Indonesia resulting from relocation up to 2016

The change in subduction pattern from oblique convergence in Sumatra to frontal convergence in southern Java results in different structural patterns and seismicity characteristics between Java and Sumatra. Seismicity recordings in the Javanese subduction zone indicate that Java is more 'quiet' than Sumatra, although large earthquakes that caused tsunamis have also occurred in the Java region, including the 7.8 M earthquake in East Java in 1994 [2] and the Mw 7.8 in Pangandaran in 2006 [3].

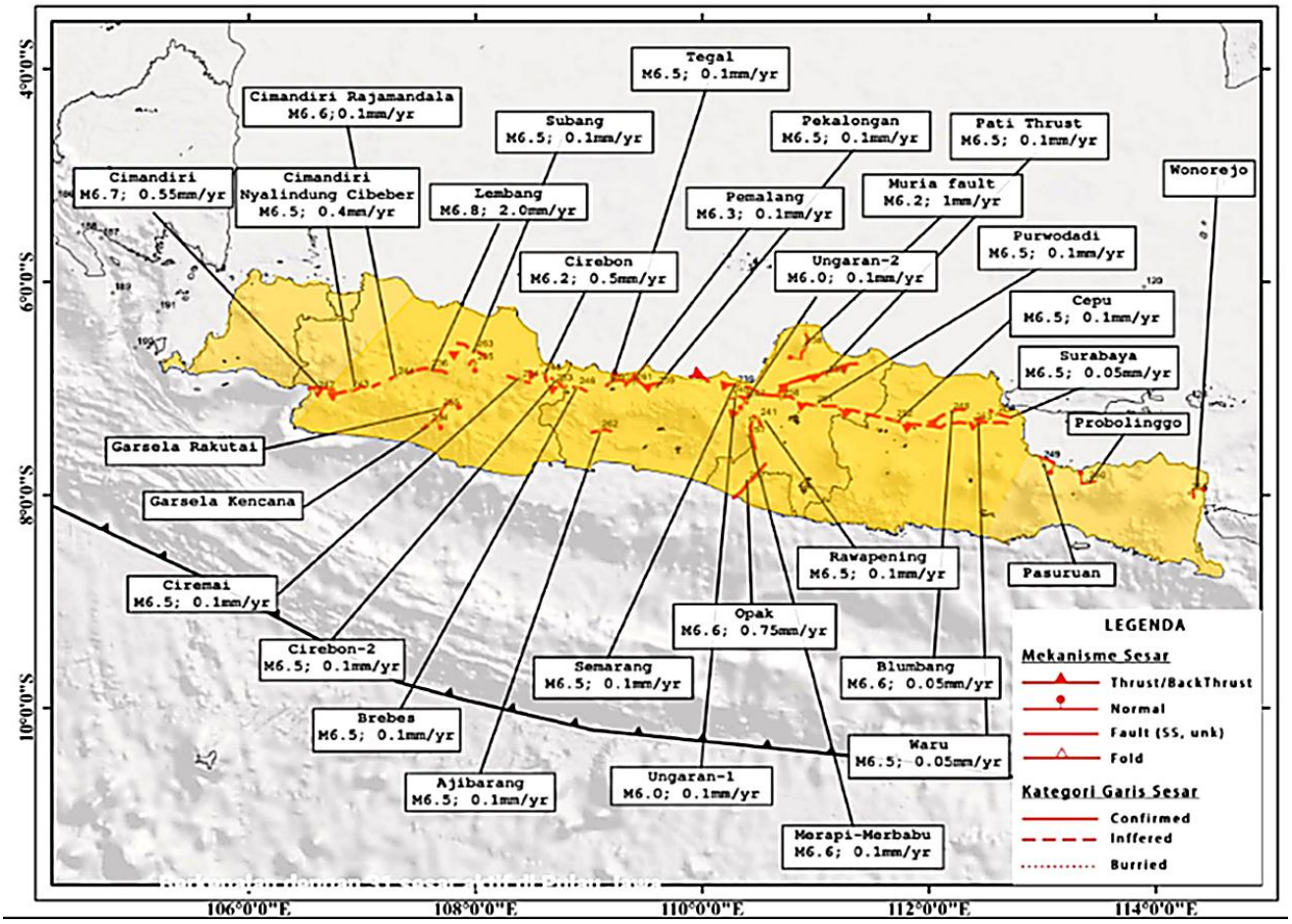

Figure 2. Active faults map in Java Island

In addition to subduction zones, shallow earthquakes originating on land have also frequently occurred in Java in recent decades. Due to Java's dense population density, these earthquakes can have quite devastating impacts. Research on mapping earthquake sources in Java, particularly active faults on land, is currently receiving attention [4]. In general, the active geological structures in Java are dominated by strike-slip faults and thrust faults with thrust faults as minor structures Some of the major faults in Java that are well known include the Cimandiri Fault [5], the Lembang Fault [6], and the Baribis-Citanduy Fault [7]. In central and eastern Java, the dominant structures are thrust faults [8](Kendeng and Semarang Fault zones), while in the eastern part of Java they are represented by a thrust fault system [9](Pasuruan, Probolinggo, and Baluran Faults). In this journal, the discussion will specifically discuss the earthquake

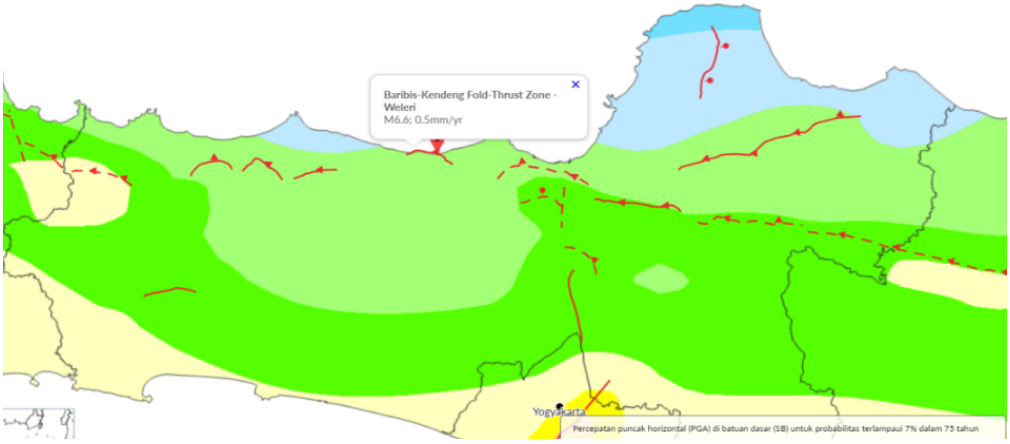

Figure 3. Baribis-kendeng fault

zone in Java, especially the Barbibis-Kendeng Fault. The Barbibis-Kendeng Fault is one of thirteen active faults along the Pantura route of Central Java as explained in Figure 3 The fault is located in Batang Regency, with a length of 17 kilometers.

Nonlinear Time History Analysis of buildings is a method that simulates the dynamic response of a structure under a given earthquake ground motion. Of all the seismic analysis methods, properly undertaken it is close to representing the reality of earthquake action on a structure [10] Earthquake acceleration time history and response spectra design are needed as basis to determine the earthquake loading that can be used to design and assess the tall building and other structures. The acceleration time history and response spectra design for certain site can be acquired using the seismic hazard analysis, amplification of ground motion quantity, and spectral matching in time domain [11]. Seismic ground motion is a key input in the seismic response history analysis for crucial engineering structures, systems and components. With the enrich of earthquake records database, conducting structural time history analysis based on real records has become an inevitable trend [12].

2. Methodogy

2.1. Overview

The development of reliable site-specific ground motion records is a fundamental step in performance-based seismic design, particularly when nonlinear dynamic (time-history) analysis is conducted. The methodology adopted in this study follows a deterministic seismic hazard analysis (DSHA) framework to define target demand spectrum, coupled with careful record selection, spectral matching (using SeismoMatch), and site response simulations to derive surface-level acceleration time histories. This integrated protocol aligns with best practices reported in the literature for constructing realistic and hazard-consistent ground motion suites [13]

2.2. Seismic Source Characterization

. The seismic source governing the hazard is the Baribis–Kendeng fault, located proximal to the study area. In line with scenario-based seismic hazard assessment frameworks such as Neo-Deterministic Seismic Hazard Assessment (NDSHA), the process begins by identifying fault parameters such as magnitude (M), rupture geometry, hypocentral and epicentral distance (R), and faulting style (strike-slip, thrust, etc.) [14] These data are critical for establishing the seismic scenario best representative of local hazard conditions.

2.3. Deterministic Attenuation Relationship and Target Spectrum

Using the identified magnitude and distance parameters, a deterministic attenuation function is developed to estimate bedrock-level peak ground acceleration (PGA) and spectrum ordinates for multiple vibration periods. This approach uses established ground motion prediction equations (GMPEs) or scenario-based attenuation models consistent with DSHA methodology [14], The computed attenuation function is then used to derive a target response spectrum (Period vs. Acceleration) representing the seismic demand at bedrock, analogous to deterministic scenario procedures described in Gediz earthquake studies [15]. Prior to using the function as a target, it is verified against regional seismic behavior and de-aggregation results of hazard data, to ensure alignment with both physical seismicity and observed attenuation trends. This step promotes consistency with best practices in local hazard validation

2.4. Record Selection from PEER NGA-West2 Database

Candidate ground motions are retrieved from the PEER NGA-West2 database by screening based on key causal parameters (Mw, R, Vs30, faulting mechanism) as seen in Figure 4. This follows recommended protocols for record selection that balance realism with spectrum shape consistency [16]

Figure 4. PEER ground database [18]

2.5. Spectral Matching via SeismoMatch

Once candidate records are selected, spectral matching is carried out using the SeismoMatch software [17], applying a tolerance level (e.g. ±10–15%) over a specified period range. This aligns selected ground motions with the target bedrock response spectrum (Period vs. Acceleration). he matched records are checked to ensure conformity to the target without introducing unrealistic spectral shapes. Selection and matching procedures echo those applied in the Italian fragility study by Selection & Match (S&M) tool, which demonstrated that strict spectral matching reduces dispersion in engineering demand prediction[18].

2.6. Site Response Analysis for Surface-Level Time Histories

To account for local geological and soil conditions, a site response (wave propagation) analysis is performed using a detailed seismic geotechnical profile (Vs30, layering, damping). This step uses 1D equivalent-linear or nonlinear software (e.g. SHAKE, DEEPSOIL) to simulate how bedrock-level motions propagate through subsurface layers, replicating site effects documented in seismically active regions. The result is a set of surface-level acceleration time histories that incorporate both target spectral demand and local amplification/de-amplification effects.

2.7. Application in Nonlinear Time-History Analysis

These site-specific surface time histories serve as input for subsequent nonlinear dynamic structural analyses (time history analysis) used to evaluate performance-based metrics such as inter-story drift, floor accelerations, plastic hinge rotations, and component demand parameters. Empirical studies on bridges and buildings (e.g., highway bridge fragility analysis, RC frame-shear wall structures) highlight the importance of carefully chosen time histories that reflect near-fault, far-field, and soil amplification characteristics in driving realistic structural responses [19]. Multiple realizations of matched records spanning M–R bins help capture record-to-record variability (RTR) and bin-to-bin variability (BTB). As demonstrated by bridge fragility studies, mismatch in record selection can significantly impact fragility curves and structural response predictions under seismic demand [20]

2.8. Integration with Performance-Based Earthquake Design

This methodology dovetails with Performance-Based Earthquake Design (PBED)frameworks in ASCE 41-17, PBED aims to design or retrofit structures so they perform in a predictable manner during earthquakes. Instead of just satisfying code minimums (like in prescriptive code design), PBED allows engineers to target performance goals (e.g., Immediate Occupancy, Life Safety, Collapse Prevention) under different earthquake hazard levels. Where achieving transparent and hazard-consistent ground motions is key. Matching records to deterministic spectra ensures the ground motion suite represents credible seismic scenarios, while site response ensures realism at the structure level.

Academic reviews have emphasized that the quality of input ground motions is critical to reliable PBED outcomes, particularly for high-importance structures (hospitals, lifelines, historic buildings) where deterministic scenarios are preferred

3. Result and Discution

3.1. Site Specific Analysis

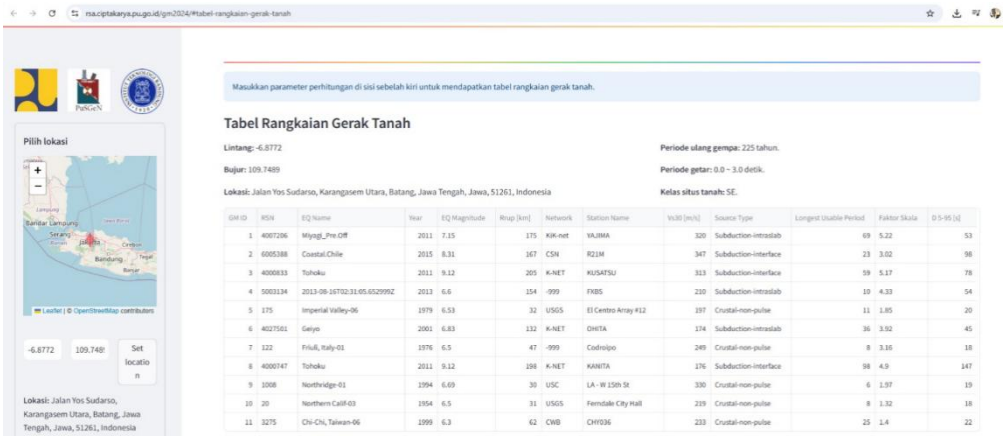

Figure 5. https://rsa.ciptakarya.pu.go.id/gm2024/ page

The steps to obtain time history loading begin with identifying the Baribis–Kendeng fault source to determine the earthquake magnitude (M), the distance from the fault to the site (R), and the fault location. Ground motion data was obtained from the page https://rsa.ciptakarya.pu.go.id/gm2024/ shown in Figure 5, where a table of ground motion data series has been provided according to earthquake parameters at the earthquake location. From the search results, seven data were obtained according to Table 1 with characteristics that are closest to the appropriate earthquake mechanism. Subsequently, after the data from acceleration time history data is obtained through the PEER Ground Motion Database to acquire seven acceleration time series data based on ground motion data from https://rsa.ciptakarya.pu.go.id/gm2024/page [8].

Table 1. Ground motion data

No	*RSN*	*EQ Name*	*Year*	*EQ Magnitude*	*Rrup [km]*	*Station Name*	*Vs30 [m/s]*	*Source Type*
1	5003134	2013-08-16T02:31:05.652999Z	2013	6.6	154	FXBS	210	*Subduction-intraslab*
2	175	Imperial Valley-06	1979	6.53	32	El Centro Array #12	197	*Crustal-non-pulse*
3	4027501	Geiyo	2001	6.83	132	OHITA	174	*Subduction-intraslab*
4	122	Friuli, Italy-01	1976	6.5	47	Codroipo	249	*Crustal-non-pulse*
5	1008	Northridge-01	1994	6.69	30	LA - W 15th St	330	*Crustal-non-pulse*
6	20	Northern Calif-03	1954	6.5	31	Ferndale City Hall	219	*Crustal-non-pulse*
7	3275	Chi-Chi, Taiwan-06	1999	6.3	62	CHY036	233	*Crustal-non-pulse*

From the SPT data, the N-SPT value can be obtained for each meter according to Table 4.2, then the soil site class can be determined according to SNI 1726-2019, where the average SPT value is in the interval 2.54 - 3.1, so it is included in the soil site class E where the average SPT value is less than 15

Table 2. Class site value

Bor Hole	*Depth*	*Soil Type*	Consitensy	N=SPT Blow	du/Ni m/Blow	N average	Class Site
BH 1	0 - 15	Clay	Very Soft	1	15	3.1	E
	15 - 18	Clay	Soft	4	0.75		
	18 - 21	Clay	Medium-Stiff	10	0.3		
	21 - 27	Clay	Stiff	13	0.46		
	27 - 30	Clay	Medium-Stiff	10	0.3		
	30 - 33	Sand	Medium-Stiff	17	0.18		
	33 - 45	Sand	Loose	10	1.2		
	45 - 60	Sand	Medium	13	1.15		
BH 2	0 - 18	Clay	Very Soft	1	18	2.84	E
	18 - 21	Clay	Soft	5	0.6		
	21 - 24	Clay	Medium-Stiff	10	0.3		
	24 - 33	Clay	Stiff	15	0.6		
	33 - 36	Clay	Very Stiff	22	0.14		
	36 - 42	Sand	Stiff	17	0.35		
	42 - 48	Sand	Very Stiff	24	0.25		
	48 - 60	Sand	Medium	14	0.86		
BH 3	0 - 21	Clay	Very Soft	1	21	2.54	E
	21 - 24	Clay	Soft	10	0.3		
	24 - 27	Clay	Medium-Stiff	14	0.21		
	27 - 30	Clay	Stiff	4	0.75		
	30 - 33	Clay	Very Stiff	6	0.5		
	33 - 36	Sand	Stiff	32	0.09		
	36 - 39	Sand	Very Stiff	16	0.19		
	39 - 42	Sand	Medium	22	0.14		
	42 - 45	Sand	Medium	19	0.16		
	45 - 60	Sand	Medium	48	0.31		
BH 4	0 - 18	Clay	Very Soft	1	18	2.74	E
	18 - 21	Clay	Medium-Stiff	7	0.43		
	21 - 27	Clay	Stiff	14	0.43		
	27 - 42	Clay	Medium-Stiff	9	1.67		
	42 - 45	Clay	Stiff	13	0.23		

	45	- 60	Sand	Medium	13	1.15		
BH 5	0	- 18	Clay	Very Soft	1	18	2.72	E
	18	- 21	Clay	Stiff	14	0.21		
	21	- 36	Clay	Very Stiff	29	0.52		
	36	- 39	Clay	Stiff	20	0.15		
	39	- 42	Clay	Very Stiff	38	0.08		
	42	- 60	Sand	Medium	14	0.86		

A deterministic attenuation function is then developed based on the values of M and R to generate Period vs. Acceleration data [9]. If, upon verification, the attenuation function is deemed appropriate, the matching of rock acceleration time history can be performed as seen in **Error! Reference source not found.**. A wave propagation analysis or site-specific analysis is conducted to obtain the acceleration time series at the site under consideration

3.2. Spectral Matching Acceleration Time History of Rocks

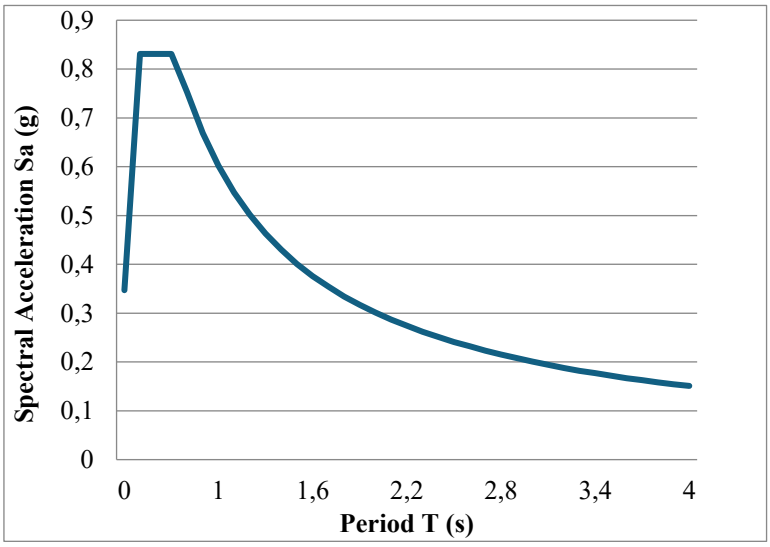

Figure 6. Design Response Spectrum Results in Batang

Time history acceleration matching is performed using the Seismo Match software program. In all three earthquake directions, data matching will be performed with the probability spectrum response as in Table 3 and Figure 6, and the spectrally matched recordings must not be less than or more than 10% of the target spectrum [21], and the results of the data matching must show convergence as shown in Table 4. Mean matched spectrum (Seismomatch)

Accelerograms	Matching	Average Multi	Maximum Multi	Iterations needed	Max Acceleration
1, IBT/NGAa	Converged	1,40%	7,20%	21	0.69107 g
1, IUS/NGAa	Converged	1,50%	10,00%	41	0.91799 g
1, V/NGAau	Converged	1,50%	8,90%	16	0.89803 g
2, IBT/RSN1	Converged	2,80%	8,60%	6	0.90645 g
2, IUS/RSN1	Converged	1,40%	6,70%	25	0.86347 g
2, V/RSN17	Converged	1,50%	5,50%	28	0.86570 g
3, IBT/NGAa	Converged	2,00%	9,50%	35	0.84734 g
3, IUS/NGAa	Converged	1,80%	8,40%	22	0.85912 g
3, V/NGAau	Converged	1,00%	7,80%	76	0.89757 g

4, IBT/RSN1	Converged	1,20%	6,90%	21	0.85474 g
4, IUS/RSN1	Converged	1,30%	7,40%	36	0.89735 g
4, V/RSN12	Converged	0,80%	5,90%	89	0.86555 g
5, IBT/RSN1	Converged	0,70%	2,90%	14	0.85240 g
5, IUS/RSN1	Converged	1,50%	7,20%	38	0.87414 g
5, V/RSN10	Converged	1,70%	9,70%	29	0.87923 g
5, IBT/RSN2	Converged	1,20%	4,80%	10	0.87262 g
6, IUS/RSN2	Converged	1,20%	8,00%	25	0.84664 g
6, V/RSN20	Converged	1,50%	6,70%	27	0.94797 g
7, IBT/RSN3	Converged	1,40%	8,60%	13	0.90699 g
7, IUS/RSN3	Converged	1,30%	9,90%	31	0.87628 g
7, V/RSN32	Converged	1,80%	9,90%	31	0.91685 g

, where the output of acceleration time histories shown in Figure 7

Table 3. Probability spectrum response in Batang

Label	As	T0	SDS	Ts	Γs+0.1	Γs+0.2	Γs+0.3	SD1	Γs+0.4	Γs+0.5	Γs+0.6	Γs+0.7	Γs+0.8	Γs+0.9	Ts+1	Ts+1.1	Ts+1.2	Ts+1.3	Ts+1.4
Period T (s)	0	0,145	0,2	0,724	0,8	0,9	1	1	1,1	1,2	1,3	1,4	1,5	1,6	1,7	1,8	1,9	2	2,1
Spectral Acceleration Sa (g)	0,347	0,831	0,831	0,831	0,753	0,669	0,602	0,602	0,547	0,502	0,463	0,43	0,401	0,376	0,354	0,334	0,317	0,301	0,287
Label	Ts+1.5	Ts+1.6	Ts+1.7	Ts+1.8	Γs+1.9	Ts+2	Γs+2.1	Ts+2.2	Ts+2.3	Γs+2.4	Ts+2.5	Ts+2.6	Γs+2.7	Γs+2.8	Γs+2.9	Ts+3	Γs+3.1	Γs+3.2	Γs+3.3
Period T (s)	2,2	2,3	2,4	2,5	2,6	2,7	2,8	2,9	3	3,1	3,2	3,3	3,4	3,5	3,6	3,7	3,8	3,9	4
Spectral Acceleration Sa (g)	0,274	0,262	0,251	0,241	0,232	0,223	0,215	0,208	0,201	0,194	0,188	0,182	0,177	0,172	0,167	0,163	0,158	0,154	0,151

Table 4. Mean matched spectrum (Seismomatch)

Accelerograms	**Matching**	**Average Multi**	**Maximum Multi**	**Iterations needed**	**Max Acceleration**
1, IBT/NGAa	Converged	1,40%	7,20%	21	0.69107 g
1, IUS/NGAa	Converged	1,50%	10,00%	41	0.91799 g
1, V/NGAau	Converged	1,50%	8,90%	16	0.89803 g
2, IBT/RSN1	Converged	2,80%	8,60%	6	0.90645 g
2, IUS/RSN1	Converged	1,40%	6,70%	25	0.86347 g
2, V/RSN17	Converged	1,50%	5,50%	28	0.86570 g
3, IBT/NGAa	Converged	2,00%	9,50%	35	0.84734 g
3, IUS/NGAa	Converged	1,80%	8,40%	22	0.85912 g
3, V/NGAau	Converged	1,00%	7,80%	76	0.89757 g
4, IBT/RSN1	Converged	1,20%	6,90%	21	0.85474 g
4, IUS/RSN1	Converged	1,30%	7,40%	36	0.89735 g
4, V/RSN12	Converged	0,80%	5,90%	89	0.86555 g
5, IBT/RSN1	Converged	0,70%	2,90%	14	0.85240 g
5, IUS/RSN1	Converged	1,50%	7,20%	38	0.87414 g
5, V/RSN10	Converged	1,70%	9,70%	29	0.87923 g
5, IBT/RSN2	Converged	1,20%	4,80%	10	0.87262 g
6, IUS/RSN2	Converged	1,20%	8,00%	25	0.84664 g
6, V/RSN20	Converged	1,50%	6,70%	27	0.94797 g
7, IBT/RSN3	Converged	1,40%	8,60%	13	0.90699 g
7, IUS/RSN3	Converged	1,30%	9,90%	31	0.87628 g

7, V/RSN32	Converged	1,80%	9,90%	31	0.91685 g

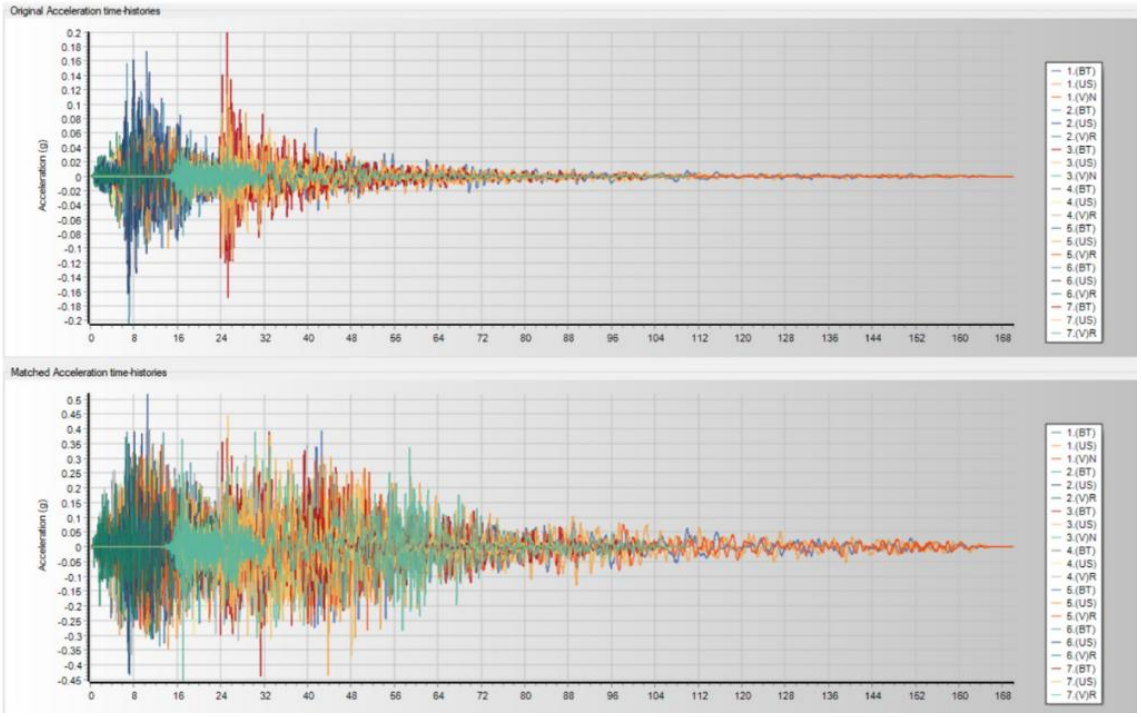

Figure 7. Output of acceleration time histories (Seismomatch)

4. Conclusions

This study presents a comprehensive methodology for site-specific seismic hazard assessment and ground motion selection, focusing on the Baribis-Kendeng Fault in Central Java, Indonesia. By integrating Deterministic Seismic Hazard Analysis (DSHA), spectral matching of ground motions, and site response analysis, the research provides a robust framework for evaluating structural performance under seismic loading.

Key findings include:

1. Seismic Hazard Characterization: The Baribis-Kendeng Fault was identified as the governing seismic source, with fault parameters (magnitude, distance, and mechanism) used to derive a deterministic target spectrum.
2. Ground Motion Selection and Matching: Seven records from the PEER NGA-West2 database were selected and spectrally matched to the target spectrum using SeismoMatch, ensuring compliance with a ±10% tolerance. This step enhanced the accuracy of the input motions for nonlinear dynamic analysis.
3. Site-Specific Effects: Subsurface soil data classified the site as Soil Class E (very soft soil), highlighting significant ground motion amplification. Site response analysis translated bedrock motions to surface-level accelerations, capturing local soil behavior.

The methodology aligns with Performance-Based Earthquake Design (PBED) principles, ensuring structures meet predefined performance objectives under seismic events. Future work could explore probabilistic seismic hazard analysis (PSHA) for a more comprehensive risk assessment and extend the framework to other seismically active regions.

This study contributes to advancing seismic design practices, offering a validated approach for engineers to enhance structural resilience in earthquake-prone areas like Indonesia.

References

[1] Tim Pusat Studi Gempa Nasional, *Peta Sumber dan Bahaya Gempa Indonesia Tahun 2017*, Bandung: Pusat Penelitian dan Pengembangan Perumahan dan Permukiman, Kementerian PUPR, 1st ed., Sep. 2017

[2] R. E. Abercrombie and G. Ekström, "Earthquake slip on oceanic transform faults," *Nature*, vol. 410, pp. 74–77, Mar. 2001

[3] C. J. Ammon, A. A. Velasco, and T. Lay, "The 17 July 2006 Java tsunami earthquake," *Geophysical Research Letters*, vol. 33, no. 15, art. L24308, 2006

[4] G. I. Marliyani, J. R. Arrowsmith, and K. X. Whipple, "Characterization of slow slip rate faults in humid areas: Cimandiri fault zone, Indonesia," *Journal of Geophysical Research: Earth Surface*, vol. 121, 2016.

[5] D. Noeradi et al., "Stress and fault system along the Cimandiri fault zone, West Java, Indonesia," *Journal of Southeast Asian Earth Sciences*, vol. 9, no. 1-2, pp. 3–11, 1994.

[6] J. A. Katili and Soetadi, "A review of the geotectonic theories of Indonesia," *Earth-Science Reviews*, vol. 7, no. 3, pp. 143–163, 1971

[7] S. Supartoyo, E. T. Putranto, and D. Djadja, "*Active Faults and Destructive Earthquake Epicenter Distribution Map of Indonesia"*, Direktorat Vulkanologi dan Mitigasi Bencana Geologi, Bandung, 2005

[8] I. Meilano, H. Z. Abidin, H. Andreas, I. Gumilar, D. Sarsito, R. Hanifa, and Y. Fukuda, "Slip rate estimation of the Lembang Fault, West Java from geodetic observation," *Journal of Disaster Research*, vol. 7, no. 1, pp. 12–18, 2012.

[9] M. M. Mukti, S. C. Singh, R. Moeremans, N. D. Hananto, H. Permana, and I. Deighton, "Neotectonics of the Southern Sumatran Forearc," in *Proc. Indonesian Petroleum Association, 36th Annual Convention and Exhibition*, 2012, Paper No. IPA12–G–074.

[10] Hashemi, Gholamreza, Shahab Ramhormozian, dan George Charles Clifton. "A Review on Nonlinear Time History Analysis of Structures." *2024 New Zealand Society for Earthquake Engineering Annual Technical Conference*, 9 Apr. 2024

[11] Makrup and A. U. Jamal, "The earthquake ground motion and response spectra design for Sleman, Yogyakarta, Indonesia with probabilistic seismic hazard analysis and spectral matching in time domain," *American Journal of Civil Engineering*, vol. 4, no. 6, pp. 298–305, 2016

[12] L. Yang, Z. Fu, dan D. Wang, "Ground motion time history simulation for seismic response history analysis," *Frontiers in Earth Science*, vol. 10, art. 908498, 9 Mei 2022

[13] D. Huang, W. Du, and H. Zhu, "A procedure to select ground motion time histories for deterministic seismic hazard analysis from the Next Generation Attenuation (NGA) database," *Natural Hazards and Earth System Sciences*, vol. 17, pp. 1725–1739, 2017

[14] G. F. Panza, A. Peresan, and E. Zuccolo, "NDSHA: Robust and reliable seismic hazard assessment," *Natural Hazards*, vol. 64, no. 1, pp. 1151–1174, 2012

[15] Ş. G. Sarp, "Application of deterministic seismic hazard analysis on the area of 1970 Gediz earthquake," *International Journal of Engineering and Applied Sciences*, vol. 5, no. 2, pp. 1–5, 2013

[16] Y. Ding, J. Zhao, X. Zhao, and Z. Zhang, "A stochastic earthquake ground motion database and its application in seismic analysis of an RC frame-shear wall structure," *Buildings*, vol. 13, no. 7, pp. 1685, 2023

[17] A.L. Atik, N. Abrahamson, "An Improved Method for Nonstationary Spectral Matching", 2010

[18] J. Hancock, J. Watson-Lamprey, and N. A. Abrahamson, “An improved method of matching response spectra of recorded earthquake ground motion using wavelets,” *Journal of Earthquake Engineering*, vol. 10, pp. 67–89, 2006.

[19] Y. Ding, Y. Xu, and S. Ding, “A stochastic earthquake ground motion database and its application in seismic analysis of an RC frame-shear wall structure,” *Buildings*, vol. 13, no. 7, art. no. 1637, 2023

[20] H. Li, G. Zhou, and J. Wang, “Selection of ground motion intensity measures and evaluation of the ground motion-related uncertainties in the probabilistic seismic demand analysis of highway bridges,” *Buildings*, vol. 12, no. 8, art. no. 1184, 2022

[21] BSN, “SNI 1726 : 2019 : Tata cara perencanaan ketahanan gempa untuk struktur bangunan gedung dan nongedung”, Jakarta, Indonesia: Badan Standardisasi Nasional , 2019